Applied Physics Letters

Indirect and direct optical transitions in $In_{0.5}Ga_{0.5}As/GaP$ quantum dots

Cite as: Appl. Phys. Lett. **104**, 123107 (2014); https://doi.org/10.1063/1.4870087
Submitted: 15 January 2014 • Accepted: 20 March 2014 • Published Online: 27 March 2014

G. Stracke, E. M. Sala, S. Selve, et al.

Indirect and direct optical transitions in $In_{0.5}Ga_{0.5}As$/GaP quantum dots

G. Stracke,[1,a)] E. M. Sala,[1] S. Selve,[2] T. Niermann,[3] A. Schliwa,[1] A. Strittmatter,[1] and D. Bimberg[1]
[1]*Institut für Festkörperphysik, Technische Universität Berlin, Hardenbergstrasse 36, 10623 Berlin, Germany*
[2]*Zentraleinrichtung Elektronenmikroskopie, Technische Universität Berlin, Straße des 17. Juni 135, 10623 Berlin, Germany*
[3]*Institut für Optik und Atomare Physik, Technische Universität Berlin, Straße des 17. Juni 135, 10623 Berlin, Germany*

(Received 15 January 2014; accepted 20 March 2014; published online 27 March 2014)

We present a study of self-assembled $In_{0.5}Ga_{0.5}As$ quantum dots on GaP(001) surfaces linking growth parameters with structural, optical, and electronic properties. Quantum dot densities from 5.0×10^7 cm^{-2} to 1.5×10^{11} cm^{-2} are achieved. A ripening process during a growth interruption after $In_{0.5}Ga_{0.5}As$ deposition is used to vary the quantum dot size. The main focus of this work lies on the nature of optical transitions which can be switched from low-efficient indirect to high-efficient direct ones through improved strain relief of the quantum dots by different cap layers. © *2014 AIP Publishing LLC*. [http://dx.doi.org/10.1063/1.4870087]

The direct-bandgap semiconductor InGaAs represents the basis of the active area of a multitude of commercial photonic devices, mostly on GaAs and InP substrates. InGaAs based quantum dots (QDs), confining charge carriers in all three dimensions of space largely improve laser properties like material gain, threshold current density, or temperature stability.[1] Recently, GaP has attracted research interest for its potential to realize defect-free III/V semiconductor heterostructures on silicon substrates.[2,3] Being an indirect semiconductor, GaP cannot serve as active medium for efficient photonic devices. Consequently, several studies of InGaAs[4–8] and InGaAsN[9] QDs on GaP have been published during the last years, including an InGaAs/GaP QD light emitting diode on Si substrate.[10] The extreme lattice mismatch of 11.2% between InAs and GaP on the one hand represents a challenge for the growth of dislocation-free QD structures. On the other hand, together with a strong quantum confinement, it produces indirect bandgaps in (In, Ga)As/GaP nanostructures,[7,11–13] yielding poor luminescence unsuited for photonic devices. Here, we report on direct-bandgap $In_{0.5}Ga_{0.5}As$/GaP(001) QDs with strong optical emission via strain engineering by different QD cap layers.

Another promising application are QD-based memory cells, combining fast access times with long retention times.[14] 1.6 s hole retention time were demonstrated for InAs/GaAs QDs with additional $Al_{0.9}Ga_{0.1}As$ barrier. In order to increase retention times decisively, little explored material combinations like InGaAs QDs in (Ga, Al)P must be considered.[15] We determined the hole retention time in $In_{0.25}Ga_{0.75}As$/GaP QDs to 3 μs,[4] more than 3 orders of magnitude longer than in InAs/GaAs QDs,[16] validating the potential of $In_xGa_{1-x}As$/(Ga, Al)P QDs as a basis for nanomemories. The retention time of charge carriers in QDs is proportional to the inverse of their capture cross-section, which varies over 3 orders of magnitude for different QD materials.[15] Yet, methods modifying the capture cross-section in favor of retention time for a given material system are still missing. The switching between indirect and direct QDs in the same material system reported in this paper allows for future studies of the impact of the electronic QD structure on the capture processes of charge carriers into QDs.

In our previous work,[4,17] we demonstrated the growth of $In_{0.25}Ga_{0.75}As$ QDs on GaP(001) by metalorganic vapour phase epitaxy (MOVPE). To initiate the three-dimensional growth (Stranski–Krastanow mode) of $In_xGa_{1-x}As$ on GaP, the GaP surface needs to be covered by 2-3 monolayers (ML) of GaAs prior to $In_xGa_{1-x}As$ deposition. Here, we present a systematic study of growth parameters affecting density and size, as well as, emission wavelength and intensity of the QDs, based on photoluminescence (PL) spectroscopy, atomic force microscopy (AFM), and transmission electron microscopy (TEM). Finally, we propose a model of the electronic structure of $In_{0.5}Ga_{0.5}As$/2.2 ML GaAs/GaP QDs based on experimental results and eight-band $\mathbf{k}\cdot\mathbf{p}$ calculations.

Samples are grown in a horizontal MOVPE reactor on GaP(001) substrates using H_2 as carrier gas. First, 500 nm thick undoped GaP buffer layers are grown at a substrate temperature of 750 °C. The temperature is then lowered to 500 °C for the growth of GaAs and $In_{0.5}Ga_{0.5}As$ layers. If not mentioned otherwise, after deposition of the $In_{0.5}Ga_{0.5}As$ layer, growth interruptions (GRI) ranging from 1 s to 400 s without any precursor supply are applied, followed by the deposition of 6 nm GaP. Buried QDs for PL and TEM measurements are additionally overgrown by 50 nm GaP at 600 °C. The TEM measurements were performed at the FEI TITAN 80–300 Berlin Holography Special operated at 300 kV.

Fig. 1 shows AFM images of samples with varying $In_{0.5}Ga_{0.5}As$ coverage on 2.2 ML GaAs/GaP. No additional cap layers were grown after $In_{0.5}Ga_{0.5}As$ deposition. For 0.42 ML $In_{0.5}Ga_{0.5}As$, the surface has a smooth two-dimensional structure (Fig. 1(a)). QD formation sets in for deposition of 0.52 ML $In_{0.5}Ga_{0.5}As$. QD densities rapidly increase from 5.0×10^7 cm^{-2} to 1.5×10^{11} cm^{-2} for increasing deposition from 0.52 ML to 0.90 ML $In_{0.5}Ga_{0.5}As$ (Fig. 1(d)). Average

a)E-mail: gernot.stracke@tu-berlin.de

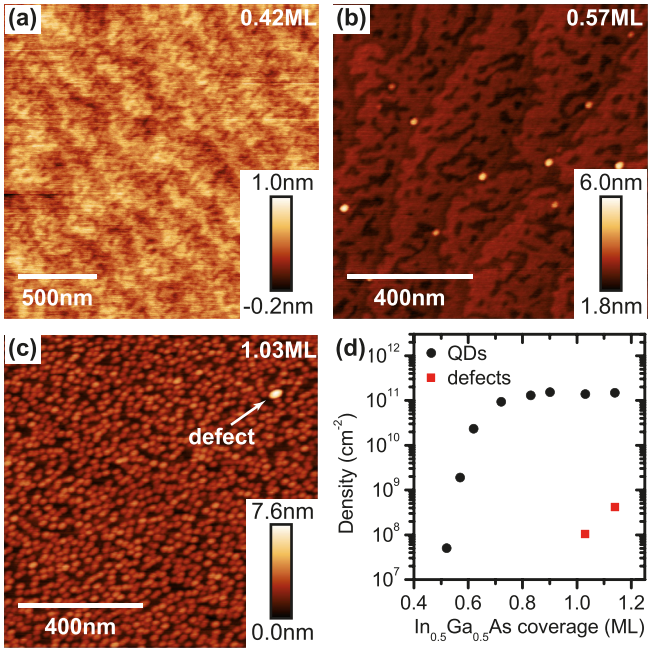

FIG. 1. AFM images of (a) 0.42 ML, (b) 0.57 ML, and (c) 1.03 ML $In_{0.5}Ga_{0.5}As$ deposited on 2.2 ML GaAs on GaP. (d) QD and defect density versus $In_{0.5}Ga_{0.5}As$ coverage.

QD height and base length are 3.1 ± 0.5 nm and 21.7 ± 2.0 nm, respectively. For >1.0 ML $In_{0.5}Ga_{0.5}As$ coverage large defective clusters are observed (Figs. 1(c) and 1(d)). The defect density is 4.2×10^8 cm^{-2} for 1.14 ML $In_{0.5}Ga_{0.5}As$. These defects have an average height and diameter of 7.6 ± 1.2 nm and 42.3 ± 2.9 nm, respectively.

Room temperature PL spectra of buried $In_{0.5}Ga_{0.5}As$ layers with varying thickness grown on 2.2 ML GaAs/GaP are shown in Fig. 2. For ≤0.41 ML $In_{0.5}Ga_{0.5}As$, the emission around 685 nm is attributed to a wetting layer (WL) formed by the GaAs and $In_{0.5}Ga_{0.5}As$ layers. The PL peak shifts abruptly to 739 nm for 0.46 ML $In_{0.5}Ga_{0.5}As$ (Fig. 2(b)), in good agreement with the onset of QD formation observed in AFM (Fig. 1). Thus, this second peak is attributed to QD luminescence and the critical $In_{0.5}Ga_{0.5}As$ coverage for QD formation is determined to 0.46 ML. Upon increasing the $In_{0.5}Ga_{0.5}As$ coverage to 1.03 ML, the QD luminescence shifts to 800 nm, and the intensity rises, reflecting increasing QD size and density also observed in AFM (Fig. 1). The integrated PL intensity plotted in the inset of Fig. 2(a) drops for >1.03 ML $In_{0.5}Ga_{0.5}As$ indicating non-radiative recombination caused by the onset of cluster formation as seen in the AFM images. Fig. 2(c) depicts the peak wavelength versus $In_{0.5}Ga_{0.5}As$ coverage.

Fig. 3 shows AFM images of two QD samples with 1.27 ML $In_{0.5}Ga_{0.5}As$/2.2 ML GaAs/GaP. The structures are capped by 6 nm GaP after a GRI without any precursor supply of 10 s and 200 s, respectively. For a GRI of 10 s, only small modulations <1 nm of the surface are visible, indicating that the underlying QDs are very small. For a GRI of 200 s, the surface exhibits distinct hills with a height of 1.3 ± 0.4 nm. This implies a ripening process during the GRI resulting in larger QDs for longer GRIs.[18] Fig. 4 shows a TEM micrograph of a sample containing 0.85 ML $In_{0.5}Ga_{0.5}As$ on 2.2 ML GaAs in GaP. The GRI was set to

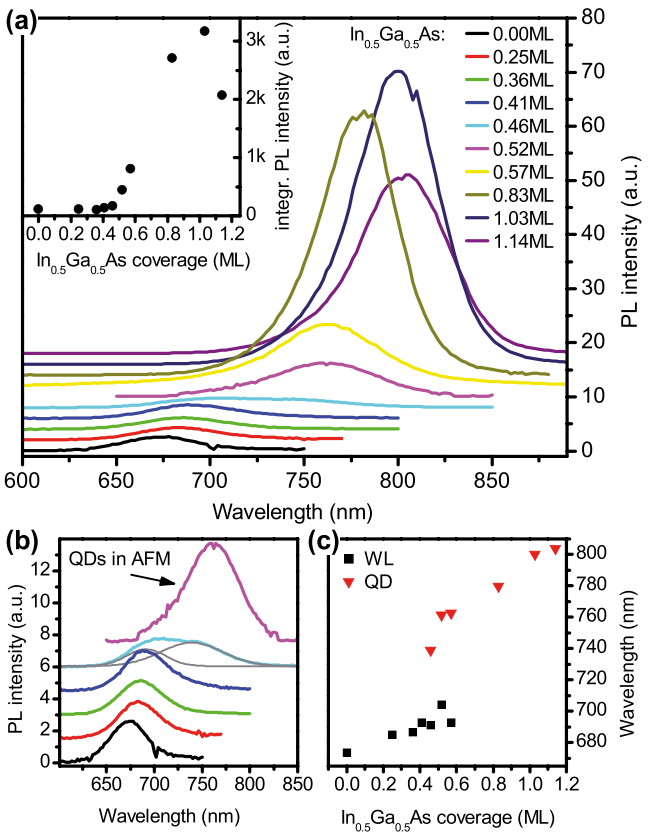

FIG. 2. (a) Room temperature PL spectra of buried $In_{0.5}Ga_{0.5}As$ layers of varying thickness on 2.2 ML GaAs/GaP. The $In_{0.5}Ga_{0.5}As$ is capped by 1.6 ML GaAs and 56 nm of GaP to improve the PL intensity (see Fig. 6). The curves are offset vertically for better visualization. The inset shows the integrated PL intensity versus $In_{0.5}Ga_{0.5}As$ coverage. (b) Spectra for low $In_{0.5}Ga_{0.5}As$ coverage of 0 to 0.52 ML reflecting the 2D-3D transition. (c) Spectral position of WL and QD PL peaks.

200 s. The micrograph was obtained under strong-beam dark field conditions using the {200} reflection in growth direction. The image intensities under these conditions are interpretable as specimen composition projected along the beam direction (InGaAs dark; GaP bright). The specimen was rotated by 13.25° with respect to the beam in order to visualize the QD in-plane distribution and avoid overlapping of several QDs in the micrograph. The QDs exhibit the typical shape[19] of a truncated pyramid and comparable size as the not-overgrown QDs.

The impact of the GRI on the QD luminescence is shown in Fig. 5 for QDs without (a) and with (b) an additional 1.6 ML

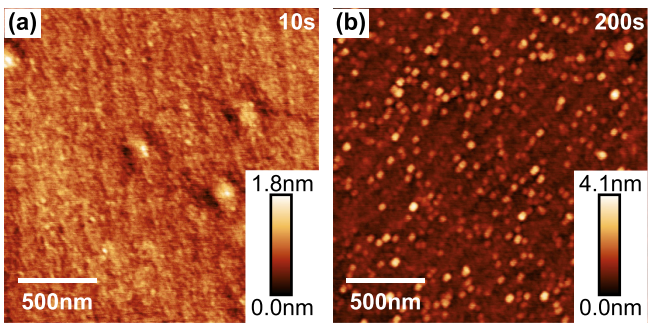

FIG. 3. AFM images of 1.27 ML $In_{0.5}Ga_{0.5}As$/2.2 ML GaAs/GaP, capped with 6 nm GaP after a GRI of (a) 10 s, (b) 200 s.

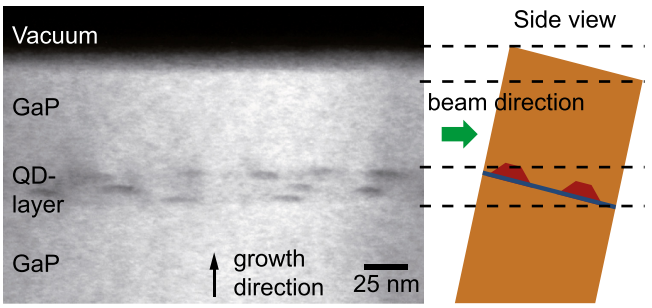

FIG. 4. Cross-sectional TEM image of 0.85 ML In0.5GaAs/2.2 ML GaAs/GaP QDs, (strong-beam {200} darkfield). Darker contrasts correspond to InGaAs rich areas. The specimen was tilted by 13.25° with respect to the beam as indicated by the sketch on the right hand side to avoid imaging overlapping QDs.

GaAs layer above the QDs. The additional GaAs layer is grown after the GRI and before the low temperature 6 nm GaP cap layer and will be motivated below. The insets show the integrated luminescence versus GRI. The luminescence of QDs without additional GaAs layer exhibits a rapid evolution of the QD luminescence intensity with the GRI duration up to 30 s and remains nearly constant up to GRIs of 300 s. The drop of the PL intensity for GRIs >300 s indicates the formation of defects. The luminescence of QDs with additional GaAs layer increases continuously with the GRI duration and reaches a maximum for a GRI of 150 s. For longer GRIs the intensity drops quickly. The luminescence of QDs with additional GaAs layer shifts from 754 nm for a GRI of 1 s to 828 nm for a GRI of 180 s. Such a red-shift for longer GRIs is also observed for InAs/GaAs QDs,[18] caused by a size increase of the QDs. For QDs without additional GaAs layer, no such wavelength shift is observed. It is noted that the additional GaAs layer is grown after the GRI and, thus, cannot influence the QD ripening during the GRI.

Fig. 6 shows PL spectra of samples containing buried 0.83 ML $In_{0.5}Ga_{0.5}As$/2.2 ML GaAs/GaP QDs capped by 1 ML to 5 ML GaAs after a GRI of 150 s, followed by 56 nm of GaP. The additional GaAs layer has strong impact on PL wavelength and intensity. The PL peak shifts from 722 nm for QDs without additional GaAs layer to 843 nm for QDs capped with additional 3 ML of GaAs. Such a red-shift can be attributed to a redistribution of the strain inside the QDs and was previously observed for InAs/GaAs QDs when overgrown with $In_xGa_{1-x}As$[20] (Dot-in-a-Well structures) or $GaAs_xSb_{1-x}$ layers.[21]

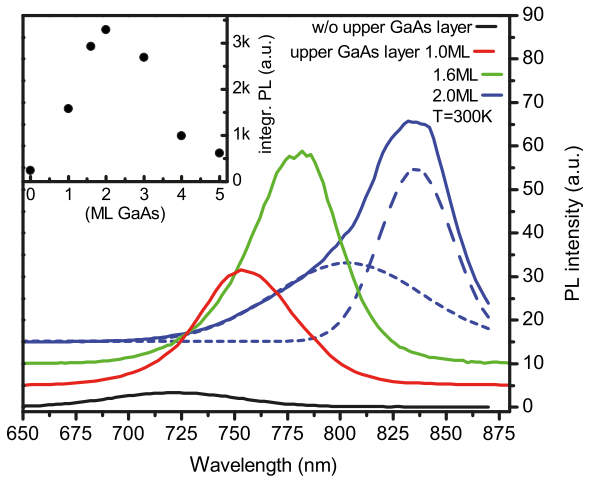

FIG. 6. Room temperature PL spectra of buried 0.83 ML $In_{0.5}Ga_{0.5}As$/2.2 ML GaAs/GaP QDs with an additional GaAs layer of varying thickness directly above the QDs. GRI = 150 s. Dotted lines represent Gaussians fitted to the data. The spectra are vertically offset for better visualization. The inset shows the integrated PL intensity versus the additional GaAs layer thickness.

The integrated PL intensity shown in the inset of Fig. 6 is 13 times higher for QDs capped with 2 ML of GaAs as compared to QDs without GaAs capping. The intensity drop for >2 ML GaAs indicates the formation of defects which might form due to the additional strain introduced to the structure by the GaAs layer.

Quantum confinement and strain effects in a QD can cause a crossing of the electronic level derived from the Γ state of the bulk material above those derived from the X and L states. Tight-binding calculations[7] of InGaAs/GaP QDs predict that for the QD size found in our work and an indium amount of 50% the Γ-derived level lies above the X- and L-derived levels, resulting in a weak overlap of electron and hole wave functions. In highly compressively strained QDs, the lowest electron level can even be pushed above that of the surrounding matrix, resulting in a type II band alignment with electrons residing in the matrix and holes in the QD.[12] If additionally the matrix has an indirect bandgap like GaP, with the lowest electron states at the X point of the Brillouin zone, the X level splits at the QD interface due to strain effects, forming a localized well for electrons at the interface of QD and matrix (Fig. 7). The resulting bandgap of the system is indirect in both real and reciprocal space. Such a switching from a direct to an indirect bandgap along

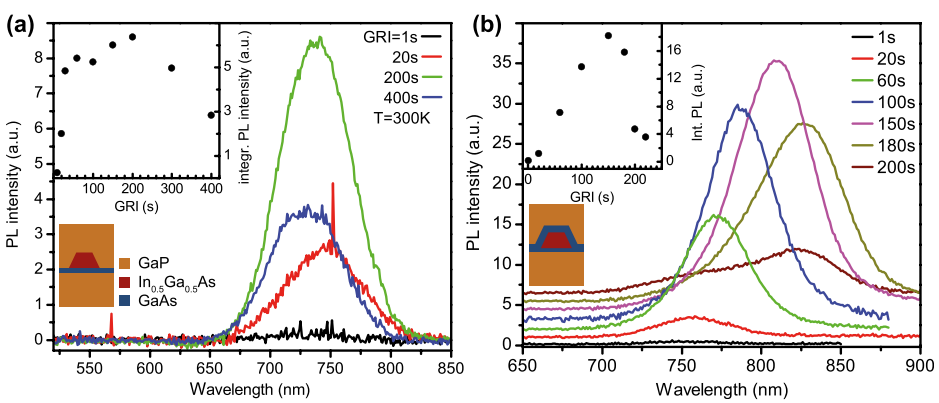

FIG. 5. Room temperature PL spectra of buried QDs with varying GRI after $In_{0.5}Ga_{0.5}As$ deposition. (a) without and (b) with additional 1.6 ML GaAs above the QDs. The spectra in (b) are vertically offset for better visualization. The insets show the integrated PL intensity versus GRI.

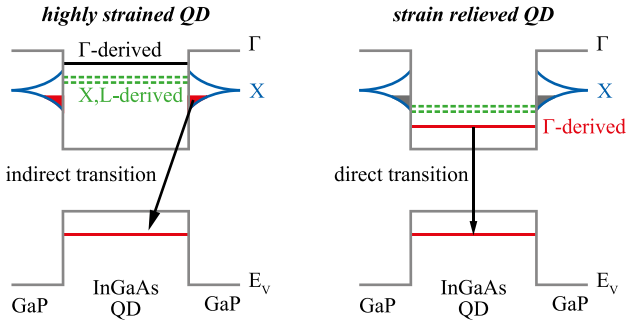

FIG. 7. Schematic of the proposed bandstructure for highly strained and strain relieved InGaAs/GaP QDs.

with a decrease in PL intensity by more than two orders of magnitude was observed for InP/GaP QDs upon increasing the pressure on the QDs.[22]

$In_{0.5}Ga_{0.5}As$/2.2 ML GaAs/GaP QDs without GaAs coverage exhibit luminescence between 1.66 eV and 1.72 eV, in good agreement with the transition energy of 1.67 eV between the GaP X valley and the QD hole level determined from eight-band **k**·**p** calculations. For the calculation, a truncated pyramid shaped $In_{0.5}Ga_{0.5}As$/2 ML GaAs/GaP QD with 12 nm base length and 10 ML height was assumed, according to the size and shape of $In_{0.25}Ga_{0.75}As$/3 ML GaAs/GaP QDs measured by cross-sectional scanning tunneling microscopy.[17] The absence of a size-dependent wavelength shift (Fig. 5) for this type of QDs supports the interpretation of an indirect type II band alignment, as the QD size has negligible impact on the GaP-X-valley to QD-hole-level transition energy.

The overgrowth of the QDs by GaAs allows for strain relief of the QDs, eventually lowering the Γ-derived electron levels in the QD below the X- and L-derived levels and below the X states in the GaP matrix. Eight-band **k**·**p** calculations yield a direct bandgap type I transition energy of 1.51 eV for $In_{0.5}Ga_{0.5}As$ QDs encapsulated in GaAs on GaP substrate. This result agrees very well with the emission at 1.48 eV from $In_{0.5}Ga_{0.5}As$/2.2 ML GaAs/GaP QDs with additional 2 ML GaAs on top. The size-dependent wavelength shift and the increased PL intensity observed for these QDs are further indications for a direct type I band alignment. Upon capping the QDs with GaAs, the PL peak splits into a doublet which can be fitted by two Gaussians, as represented by the dotted lines in Fig. 6 for 2 ML GaAs capping, indicating that additional recombination channels are being activated or a bimodal QD distribution exists.

In conclusion, we have studied in detail $In_{0.5}Ga_{0.5}As$/2.2 ML GaAs/GaP QDs grown by MOVPE. The critical coverage for QD formation is determined to 0.46 ML $In_{0.5}Ga_{0.5}As$ on 2.2 ML GaAs on GaP. The QD density lies between 5.0×10^7 cm^{-2} and 1.5×10^{11} cm^{-2} depending on the deposited $In_{0.5}Ga_{0.5}As$ amount. During a GRI after $In_{0.5}Ga_{0.5}As$ deposition, a ripening of the QDs leading to increasing QD size is observed. Improved relief of the high strain in the InGaAs/GaP QD system is achieved by introduction of a thin GaAs layer directly above the QDs. The strain relief results in a strong red-shift of the QD luminescence and an increase of the luminescence intensity by more than one order of magnitude. These effects can be explained by a strain induced switching between indirect and direct band alignment both in real and reciprocal space, thus proving the importance of strain engineering for device fabrication using InGaAs/GaP QDs.

The authors thank the DFG (Contract No. BI284/29-1), the Federal Ministry of Economics and Technology (BMWi) (Grant No. 03VWP0059v), and the Federal Ministry of Education and Research (Grant No. 16V0196 (HOFUS)).

[1]D. Bimberg, Electron. Lett. **44**, 168 (2008).
[2]A. Beyer, J. Ohlmann, S. Liebich, H. Heim, G. Witte, W. Stolz, and K. Volz, J. Appl. Phys. **111**, 083534 (2012).
[3]T. J. Grassman, J. A. Carlin, B. Galiana, L.-M. Yang, F. Yang, M. J. Mills, and S. A. Ringel, Appl. Phys. Lett. **102**, 142102 (2013).
[4]G. Stracke, A. Glacki, T. Nowozin, L. Bonato, S. Rodt, C. Prohl, A. Lenz, H. Eisele, A. Schliwa, A. Strittmatter, U. W. Pohl, and D. Bimberg, Appl. Phys. Lett. **101**, 223110 (2012).
[5]R. Leon, C. Lobo, T. P. Chin, J. M. Woodall, S. Fafard, S. Ruvimov, Z. Liliental-Weber, and M. A. S. Kalceff, Appl. Phys. Lett. **72**, 1356–1358 (1998).
[6]K. Rivoire, S. Buckley, Y. Song, M. L. Lee, and J. Vučković, Phys. Rev. B **85**, 045319 (2012).
[7]C. Robert, C. Cornet, P. Turban, T. N. Thanh, M. O. Nestoklon, J. Even, J. M. Jancu, M. Perrin, H. Folliot, T. Rohel, S. Tricot, A. Balocchi, D. Lagarde, X. Marie, N. Bertru, O. Durand, and A. Le Corre, Phys. Rev. B **86**, 205316 (2012).
[8]T. Miyamoto, S. Tanabe, R. Nishio, Y. Kobayashi, and R. Suzuki, Jpn. J. Appl. Phys., Part 1 **51**, 080201 (2012).
[9]K. Umeno, Y. Furukawa, N. Urakami, R. Noma, S. Mitsuyoshi, A. Wakahara, and H. Yonezu, Phys. E **42**, 2772–2776 (2010).
[10]Y. Song and M. L. Lee, Appl. Phys. Lett. **103**, 141906 (2013).
[11]S. Fuchi, Y. Nonogaki, H. Moriya, A. Koizumi, Y. Fujiwara, and Y. Takeda, Phys. E **21**, 36–44 (2004).
[12]A. J. Williamson, A. Franceschetti, H. Fu, L. W. Wang, and A. Zunger, J. Electron. Mater. **28**, 414–425 (1999).
[13]C. Robert, M. O. Nestoklon, K. P. da Silva, L. Pedesseau, C. Cornet, M. I. Alonso, A. R. Goñi, P. Turban, J.-M. Jancu, J. Even, and O. Durand, Appl. Phys. Lett. **104**, 011908 (2014).
[14]A. Marent, T. Nowozin, M. Geller, and D. Bimberg, Semicond. Sci. Technol. **26**, 14026 (2011).
[15]T. Nowozin, D. Bimberg, K. Daqrouq, M. N. Ajour, and M. Awedh, J. Nanomater. **2013**, Article ID 215613 (2013).
[16]M. Geller, E. Stock, C. Kapteyn, R. Sellin, and D. Bimberg, Phys. Rev. B **73**, 205331 (2006).
[17]C. Prohl, A. Lenz, D. Roy, J. Schuppang, G. Stracke, A. Strittmatter, U. W. Pohl, D. Bimberg, H. Eisele, and M. Dähne, Appl. Phys. Lett. **102**, 123102 (2013).
[18]K. Pötschke, L. Müller-Kirsch, R. Heitz, R. L. Sellin, U. W. Pohl, D. Bimberg, N. Zakharov, and P. Werner, Phys. E **21**, 606–610 (2004).
[19]A. Lenz, R. Timm, H. Eisele, C. Hennig, S. K. Becker, R. L. Sellin, U. W. Pohl, D. Bimberg, and M. Dähne, Appl. Phys. Lett. **81**, 5150 (2002).
[20]F. Guffarth, R. Heitz, A. Schliwa, O. Stier, N. Ledentsov, A. Kovsh, V. Ustinov, and D. Bimberg, Phys. Rev. B **64**, 085305 (2001).
[21]A. Hospodková, M. Zíková, J. Pangrác, J. Oswald, K. Kuldová, J. Vyskočil, and E. Hulicius, J. Cryst. Growth **370**, 303–306 (2013).
[22]A. Goñi, C. Kristukat, F. Hatami, S. Dreßler, W. Masselink, and C. Thomsen, Phys. Rev. B **67**, 075306 (2003).